

## Programming multicolour micro-patterns via regional polymer stabilized heliconical soft architecture

Bing-Hui Liu, Cong-Long Yuan, Hong-Long Hu, Pei-Zhi Sun, Li-Hong Yu and Zhi-Gang Zheng

### S1. Optimal experiment

To obtain an electric field induced heliconical structure at room temperature (26.0 °C) in the polymerizable liquid crystal (LC) system, the concentrations of traditional nematic LC E7 and LC dimer CB7CB were optimized (Table S1), where E7 possessed low clearing point (60.0 °C) and CB7CB presented a nematic phase between 104.1 °C and 117.3 °C sandwiched between the twist-bend nematic ( $N_{TB}$ ) and the isotropic phase. Considering that the sufficiently low value of bend elastic constant  $K_{33}$  in the LC system containing LC dimer was obtained only in the temperature range close to the phase transition temperature  $T_{TB}^1$ , the sample C3(R3) with 50.7 wt % E7 presenting a cholesteric phase between 23.9 °C and 73.0 °C (Fig. S1) was suitable for forming the heliconical structure, in which the phase transition temperature  $T_{tb}$  (23.9 °C) was closed to the room temperature 26.0 °C. Furthermore, the concentration of reactive monomer RM257 was optimized (Table S2). When the monomer concentration was 3.0 wt% (Sample R2), the polymer-stabilized pattern showed inconsistent size with the light-transmitting region of a periodic stripe pattern (stripe width: 160  $\mu\text{m}$ , period: 320  $\mu\text{m}$ ) after UV exposing at 8.0  $\text{mW cm}^{-2}$  for 80 s (Fig. S2). When RM257 concentration was 2.3 wt% (Sample R1), the polymer network could not remain the heliconical structure due to the insufficient anchoring effect in the absence of applied electric field. The appropriate size of stabilized pattern was enabled with increasing the RM257 concentration to 3.3 wt% (Sample R3(C3)). Therefore, the optimal weight ratio of E7:CB7CB:R811:RM257:IRG184 was 50.7:41.5:3.5:3.3:1.0. Through a similar process, the optimal ratio for E7:CB7CB:R811:RM257:PI819 was confirmed to be 50.7:42.0:3.5:3.3:0.5.

**Table S1.** The compositions of Sample C1-C5 for optimizing the concentrations of E7 and CB7CB.

Sample ID	CB7CB	E7	R811	RM257	IRG184
Sample C1	31.5 wt%	60.7 wt%	3.5 wt%	3.3 wt%	1.0 wt%
Sample C2	36.5 wt%	55.7 wt%	3.5 wt%	3.3 wt%	1.0 wt%
Sample C3(R3)	41.5 wt%	50.7 wt%	3.5 wt%	3.3 wt%	1.0 wt%
Sample C4	46.5 wt%	45.7 wt%	3.5 wt%	3.3 wt%	1.0 wt%
Sample C5	51.5 wt%	40.7 wt%	3.5 wt%	3.3 wt%	1.0 wt%

**Table S2.** The composition of Sample R1-R3 for optimizing the concentration of RM257.

Sample ID	CB7CB	E7	R811	RM257	IRG184
Sample R1	41.5 wt%	51.7 wt%	3.5 wt%	2.3 wt%	1.0 wt%
Sample R2	41.5 wt%	51.0 wt%	3.5 wt%	3.0 wt%	1.0 wt%
Sample R3(C3)	41.5 wt%	50.7 wt%	3.5 wt%	3.3 wt%	1.0 wt%

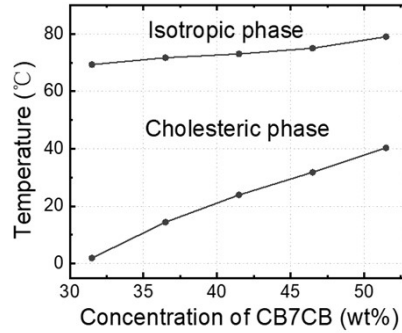


Fig. S1. Phase diagram of Sample C1-C5 depending on the concentrations of E7 and CB7CB.

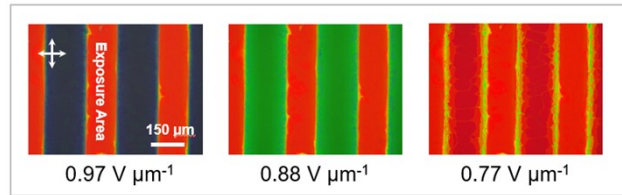


Fig. S2. The POM textures of the regional PSLC with increasing electric field of Sample R2. The red exposed area was narrower than the width of light-transmitting region (160 μm) of the photomask. The scale bar represents 150 μm.

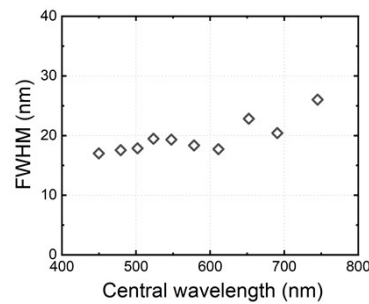


Fig. S3. The full width at half maxima (FWHM) of the reflection bands in the heliconical structure.

## S2. Grating generation

The photomask showed a pattern of binary fork grating. Here, the grating pattern was generated<sup>2</sup> by stacking phase of  $q$ -plate and polarization grating based on the Equation (S1).

$$\phi(x, y) = m \arctan \frac{y}{x} + \frac{2\pi x}{P} \quad (\text{S1})$$

---

Where  $\phi(x, y)$  was the phase distribution of fork grating in the  $x$ - $y$  plane, the first item on the right showed the phase distribution of  $q$ -plate at  $q=m/2$ ,  $m$  was topological charge, the second item showed the phase distribution of polarization grating and  $P$  was the period. Furthermore, the binary fork grating at  $m=1$  was obtained as Fig. S4, where the black region was designed as the light-transmitting region of the photomask.

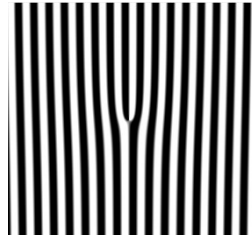


Fig. S4. The binary fork grating calculated according to Equation (S1).

### S3. Supplementary Experiment

To further characterize the polymerization results, a regional polymerized sample was immersed in dichloromethane for 10 hours to wash out the LC host, oligomers, and unpolymerized monomers. Then, the sample was placed on the hot stage at 50 °C for 30 minutes to remove the residue solvent, leaving behind the patterned polymer in the LC cell. As shown in Fig. S5, the micrograph with 20× and 100× objective respectively of the cell presented the consistent stripe size with the photomask due to the patterned polymer distribution in the cell, which further indicates that polymerization of RM257 occurs.

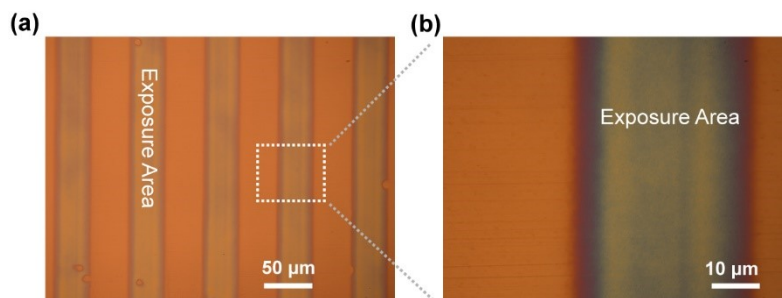


Fig. S5 The micrograph of patterned polymer distribution of regional polymerized sample observed with (a) 20× and (b) 100× objective respectively.

The micropatterns pattern in Fig. 2e contains a stabilized colour and a drivable colour. The colour change of the micropattern takes a relatively long time at a given electric field due to the assembling and constructing of the chiral structures. For example, the green structural colour (at  $0.65 \text{ V } \mu\text{m}^{-1}$ ) switches into saturated (90% of the maximum reflection) reflective red colour (at  $0.52 \text{ V } \mu\text{m}^{-1}$ ) within about 38 s; the time was measured by monitoring the reflection spectra of the sample at a time interval of 2.5 s (Fig. S6).

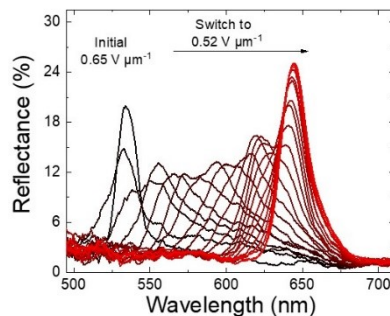


Fig. S6 The reflection band switch in the drivable area of the sample at a given electric field. The spectra were collected at a time interval of 2.5 s.

In the 12- $\mu\text{m}$ -thick LC cell, the arrangement of LC molecules existed some defects and microdomains after the UV photopolymerization, and the edge of the polymer pattern was not sharp enough. Such defects and domains could be restrained effectively by employing a thinner (4  $\mu\text{m}$ ) cell with parallel alignment. In addition, the center wavelengths of the reflection bands before UV exposure were almost consistent with those after polymerization in the thinner cell. As shown in Fig. S7a, when a square wave electric field at  $0.86 \text{ V } \mu\text{m}^{-1}$  and 1.0 kHz was applied to the prepared sample, a green planar texture appeared corresponding to heliconical arrangement, and the central wavelength of the reflection band is about 558.8 nm. When the sample was exposed with the fork grating photomask by the UV lamp ( $1.5 \text{ mW cm}^{-2}$  for 100 s), the central wavelength was 559.2 nm, i.e., the band shifted less than 0.5 nm due to low UV power density and thus no significant heating (Fig. S7b). Furthermore, the combination of coexisting structural colors was dynamically modulated, and the reversible switch between the patterned dual structural colors coexistence state and single structural color state of the heliconical structure was achieved (Fig. S7c), which were similar to that in the 12- $\mu\text{m}$ -thick LC cell described above. In addition, when an electric field strength of  $0.93 \text{ V } \mu\text{m}^{-1}$  was applied to the unexposed sample, the sample exhibited a uniform red planar texture (Fig. S7d); when the electric field strength was enhanced to  $1.11 \text{ V } \mu\text{m}^{-1}$ , the sample presented a blue texture (Fig. S7e), thereby the corresponding red or blue patterned polymer stabilized structures could be obtained by UV exposure, respectively. Compared to the sample in the 12- $\mu\text{m}$ -thick cell, the pattern edge in the 4- $\mu\text{m}$ -thick cell was sharper and the texture showed fewer defects.

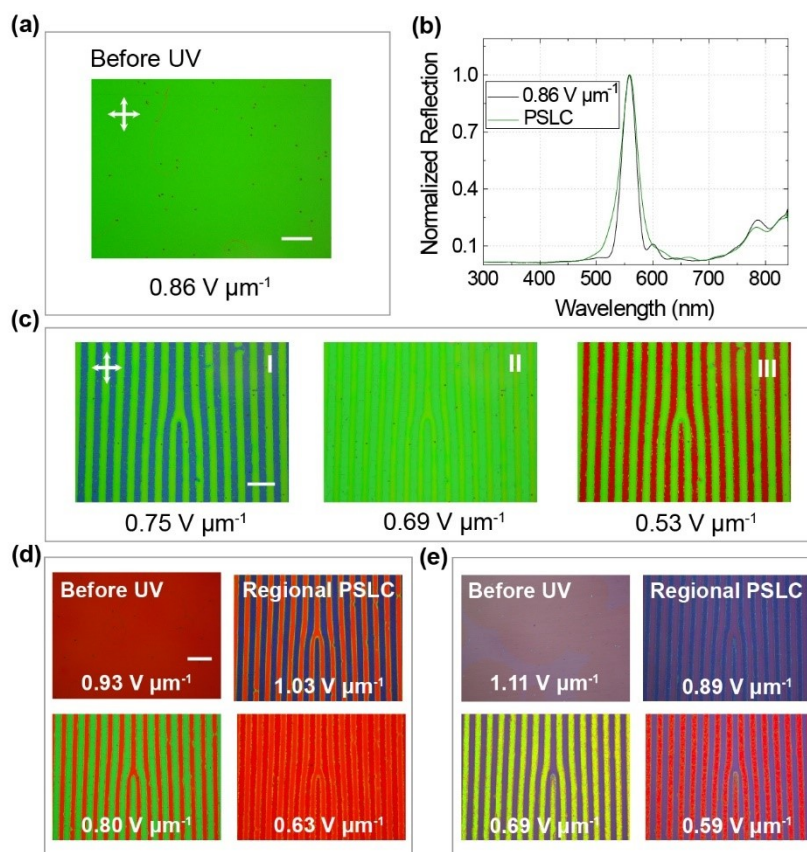


Fig. S7 (a) The POM textures of the heliconical LC system in a 4- $\mu\text{m}$ -thick cell at  $0.86 \text{ V } \mu\text{m}^{-1}$ . (b) The corresponding spectra before and after regional UV exposure. (c) The textures of the regional PSLC with increasing electric field. (d) POM textures of the heliconical LC system before UV exposure (d) at  $0.93 \text{ V } \mu\text{m}^{-1}$  and (e) at  $1.11 \text{ V } \mu\text{m}^{-1}$  respectively, and the corresponding textures of the regional PSLC with decreasing electric field. The scale bar represents  $100 \mu\text{m}$ .

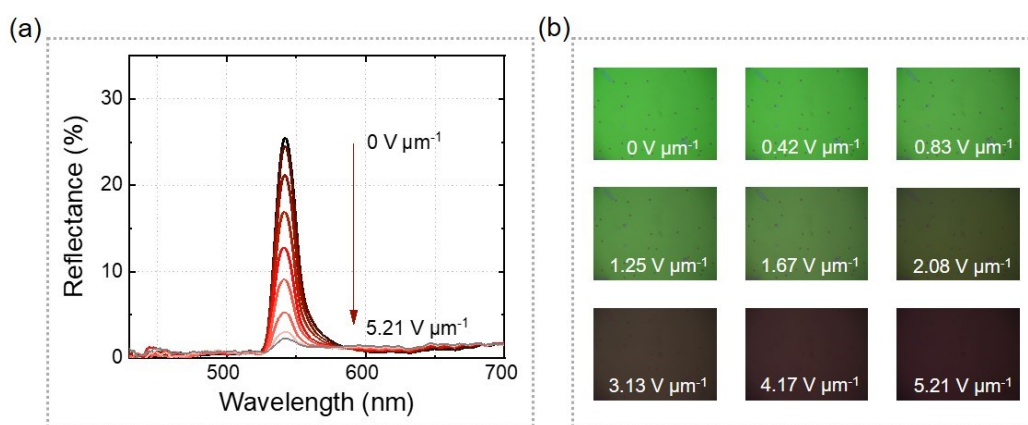


Fig. S8. The reflectance of the polymer stabilized structure gradually decreased with further increasing applied electric field strength.

In order to estimate the response times of the polymer stabilized device, the transmission intensity of a He-Ne laser beam passing through the sample (with the central wavelength of reflection band at  $633 \text{ nm}$ ) is monitored. Specifically, for the sample at  $4.33 \text{ V } \mu\text{m}^{-1}$ , 90% of the signal change was observed within  $6.7 \text{ ms}$  after the field

was switched off and 0.2 ms when the field was applied (Fig. S9).

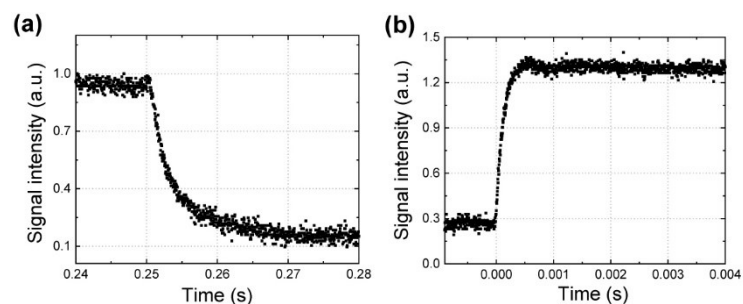


Fig. S9 Electro-optic response of a polymer stabilized sample. An electric field ( $4.33 \text{ V } \mu\text{m}^{-1}$ , square wave at 1 kHz) was turned off (a) and on (b).

When a sufficiently high electric field is applied to the patterned samples, the field-induced Fréedericksz transition unwinds the heliconical structure and the LC molecules tend to align with the field, so that the patterns are erased and present the dark states. As the electric field strength was reduced, the anchoring effect of the polymer restores the heliconical structure and the patterns reappear (Fig. S10).

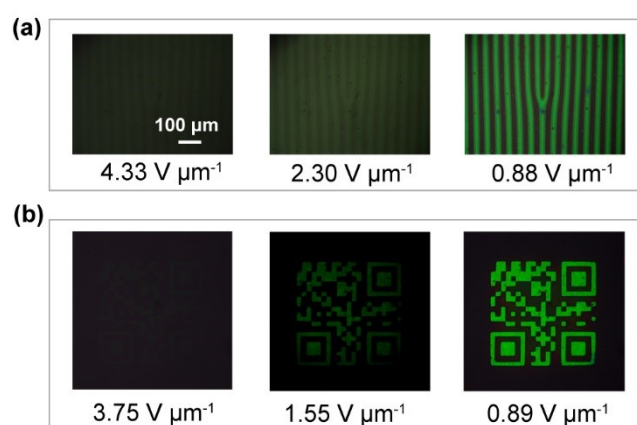


Fig. S10 The POM textures of erased micro-patterns reappearing with decreasing electric field strength.

## References

1. M. Mrukiewicz, O. S. Iadlovská, G. Babakhanova, S. Siemianowski, S. V. Shiyonovskii and O. D. Lavrentovich, *Liq. Cryst.*, 2019, **46**, 1544-1550.
2. P. Chen, B. Y. Wei, W. Ji, S. J. Ge, W. Hu, F. Xu, V. Chigrinov and Y. Q. Lu, *Photonics Res.*, 2015, **3**, 133-139.